A CPT-based Cs vapor cell atomic clock with a short-term fractional frequency stability of $3 \times 10^{-13}\ \tau^{-1/2}$

Moustafa Abdel Hafiz[1], **Xiaochi Liu**[1⋆], **Stéphane Guérandel**[2], **Emeric De Clercq**[2], **Rodolphe Boudot**[1]

[1]FEMTO-ST, CNRS, UFC, 26 chemin de l'épitaphe 25030 Besançon cedex, France.
[2]LNE-SYRTE, Observatoire de Paris, PSL Research University, CNRS, Sorbonne Universités, UPMC Univ. Paris 06, 61 avenue de l'Observatoire, 75014 Paris, France.
[⋆]now in National Institute of Standards and Technology (NIST), Boulder, CO 80305, USA.

E-mail: `rodolphe.boudot@femto-st.fr`

Abstract. This article reports on the development and short-term fractional frequency stability of a continuous-regime (CW) Cs vapor cell atomic clock based on coherent population trapping (CPT). The push-pull optical pumping technique is used to increase the number of atoms that participate to the clock transition, yielding a typical CPT resonance contrast of 25 % for a CPT linewidth of about 450 Hz. The clock short-term fractional frequency stability is measured to be $3 \times 10^{-13}\ \tau^{-1/2}$ up to 100 seconds averaging time, in correct agreement with the signal-to-noise ratio limit. The mid-term frequency stability results are currently mainly limited by laser power effects. The detection of high-contrast narrow Raman-Ramsey fringes is demonstrated with this setup by making the atoms interact with a light pulse sequence.

1. Introduction

The development of high-performance, compact and low-power consuming atomic clocks is of great interest in numerous scientific and industrial fields including new-generation satellite-based navigation systems, network synchronization, timekeeping applications or defense systems. Vapor cell atomic clocks, basically based on the combination of a laser system and thermal alkali atoms confined in a glass vapor cell, are in that sense an attractive technology to propose simultaneously simple architecture and high-performance. Over the last years, thanks to the use of better performing laser sources and dedicated techniques, laboratory-prototype vapor cell atomic clocks, based on optical-microwave double resonance technique [1, 2] or coherent population trapping (CPT) [3], have demonstrated short-term fractional frequency stability in the $1-4\times10^{-13}\ \tau^{-1/2}$ range [4, 5, 6, 7, 8]. These performances are about two orders of magnitude better than current commercially-available Rb clocks and tend to be competitive with those of passive hydrogen masers.

In the frame of the MClocks project [9], we recently started the development of a compact Cs CPT atomic clock based on the push-pull optical pumping (PPOP) technique, pioneerly proposed by Jau et al. [10]. In recent literature, we reported the spectroscopy of high-contrast CPT resonances in Cs vapor cells [11] and demonstrated the possibility to detect high-contrast Raman-Ramsey fringes [12]. This article aims to report short-term frequency-stability results of

Journal of Physics: Conference Series **723** (2016) 012013 doi:10.1088/1742-6596/723/1/012013

our CPT-PPOP based Cs vapor cell atomic clock. A promising short-term fractional frequency stability of $3 \times 10^{-13}\ \tau^{-1/2}$ up to $\tau = 100$ s integration time in CW regime, in correct agreement with the noise budget, is demonstrated.

2. Experimental setup

Figure 1 presents the Cs CPT clock experimental set-up.

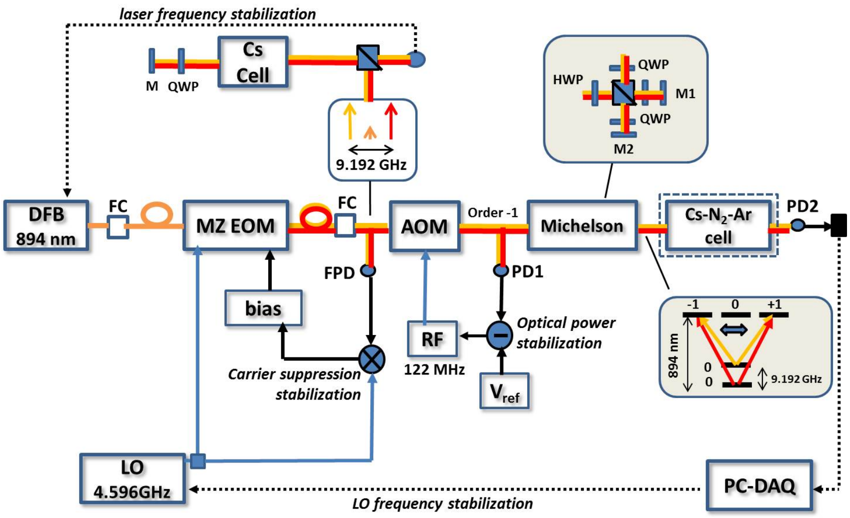

Figure 1. Schematic of the Cs vapor cell atomic clock based on push-pull optical pumping. DFB: Distributed feedback diode laser, FC: fiber collimator, MZ EOM: Mach-Zehnder electro-optic modulator, AOM: acousto-optic modulator, LO: microwave local oscillator, FPD: fast photodiode, PD: photodiode, RF: radiofrequency source, V_{ref}: reference voltage, Michelson: Michelson-type delay-line and polarization orthogonalizer system, PC-DAQ: personal computer - data acquisition card, M: mirror, QWP: quarter-wave plate, HWP: half-wave plate. An inset shows the CPT diagram involved in the push-pull optical pumping technique. A second inset shows the Michelson delay-line system principle.

The laser source is a commercially-available GaAs semi-conductor 1 MHz-linewidth distributed-feedback (DFB) diode laser tuned at 894 nm on the Cs D_1 line [13]. A Faraday optical isolator (not shown on Fig. 1) is placed at the output of the DFB laser in order to avoid optical feedback. A MZ EOM (Photline NIR-MX800-LN-10) driven at 4.596 GHz with a low noise microwave frequency synthesizer is used to generate phase-coherent optical sidebands frequency-separated by 9.192 GHz. The local oscillator consists of a high-spectral purity 100 MHz quartz-crystal oscillator phase-locked to a high-stability 10 MHz quartz source and then frequency-multiplied to 4.596 GHz. At the output of the EOM, optical carrier rejection is actively stabilized thanks to an original microwave synchronous detector presented in [11]. The laser beam that carries both optical lines frequency-split by 9.192 GHz, is sent into an annex reference Cs cell to stabilize the laser frequency using a saturated absorption spectroscopy setup. The laser is frequency-stabilized by modulating the DFB laser current at 62 kHz and demodulating it with a lock-in amplifier LA1. The laser frequency servo bandwidth is about 1.5 kHz. At the output of the EOM, an AOM-based laser power stabilization system with a servo bandwidth of about 20 kHz is implemented. The order −1 at the output of the AOM is sent to the CPT cell to shift the laser frequency by −122 MHz and to compensate for the buffer-gas induced optical frequency shift. At the output of the AOM, a Michelson delay-line and polarization orthogonalizer system is used to produce the PPOP scheme [10]. At the output of the Michelson system, the diameter beam is expanded to 2 cm. The CPT cell consists of a 2-cm diameter and 5-cm long cylindrical Cs vapor cell filled with a N_2-Ar buffer gas mixture of total pressure 15.3 Torr and partial pressure ratio $r = P_{Ar}/P_{N_2} = 0.4$. In clock operation, the cell temperature T_{cell} is stabilized at about 35°C where the CPT signal height is maximized. The presence of buffer gas in the CPT cell causes a collisional frequency shift of the Cs clock transition of about 9.3 kHz. A static magnetic field of 89 mG parallel to the laser beam propagation direction is applied to split the hyperfine ground-state Zeeman transitions. The ensemble is surrounded by a double-layer mu-metal magnetic shield. The CPT resonance is monitored by detecting the laser power transmitted through the cell using the low-noise photodiode PD2. The resulting signal is analyzed by a computer that drives the local oscillator frequency. For frequency stability measurements, the clock output signal is compared to the signal of a state-of-the-art reference active hydrogen maser that exhibits a fractional frequency stability of 8×10^{-14} and 3×10^{-15} at $\tau = 1$ s and 100 s respectively [14].

3. Frequency stability

Figure 2(a) reports the typical clock signal for an incident laser power P_L of 475 μW in the 5-cm long cell.

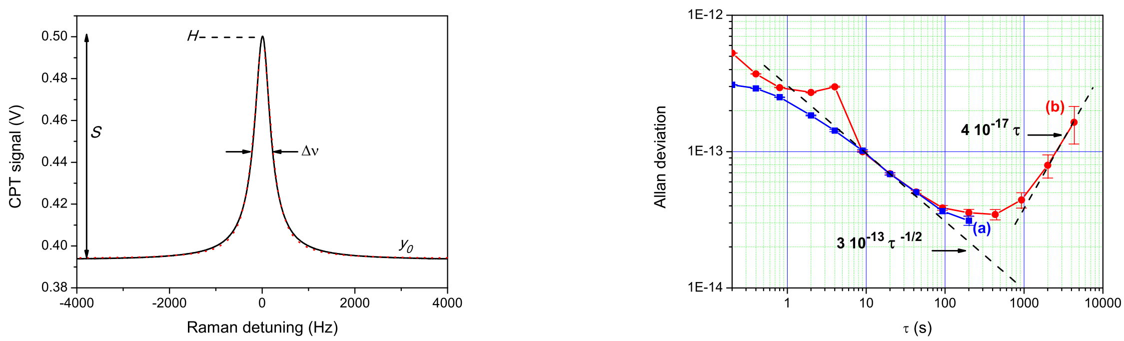

(a) (b)

Figure 2. (a): Clock CPT resonance signal. Experimental data of the direct CPT resonance are fitted by a lorentzian fit function. The total laser power incident on the cell is 475 μW. The CPT linewidth is 453 Hz. The resonance contrast is 26.4 %. (b): Allan deviation of the clock frequency. The laser power incident on the cell is 475 μW. The static magnetic field is 89 mG. (a): EOM bias servo loop off, (a): EOM bias servo loop activated. The first dashed line is a curve with a $3 \times 10^{-13}\ \tau^{-1/2}$ slope. The second dashed line is a linear curve with a slope of about $4 \times 10^{-17}\ \tau$ slope.

The clock resonance is well-fitted by a lorentzian function. The CPT linewidth $\Delta\nu$ is 453 Hz. The clock signal S, defined on Fig. 2(a) as $S = H - y_0$, is 0.104 V. The resonance contrast C, defined as the ratio between the CPT signal S and the dc background y_0, is 26.4 %. The discriminator slope $D = S/\Delta\nu$ is measured to be 2.3×10^{-4} V/Hz. Figure 2(b) shows the measured short-term fractional frequency stability of the CPT clock. In normal operation (curve b), the latter is measured to be $3 \times 10^{-13}\ \tau^{-1/2}$ up to about 100 s averaging time, in correct agreement with SNR measurements. The bump between 1 and 10 s is attributed to the EOM bias voltage servo loop gain. We suspect that this issue could prevent to observe the expected calculated short-term stability of 2×10^{-13} (see table 1). In the case where this servo is off (Fig. 2(b), curve a), the bump between 1 and 10 s clearly disappears. For integration times higher than 10 s, the observed difference between the two stability curves are within the measurement error bars. After 100 s (see curve b), the clock frequency drifts to reach 2×10^{-13} at 5000 s.

Table 1. Main contributions to the clock short term frequency stability at $\tau = 1$ s.

Noise Source	σ (1 s)
Shot noise	8×10^{-15}
Detector noise	2×10^{-14}
LO phase noise	1.1×10^{-13}
Total laser noise (AM and FM-AM)	1.7×10^{-13}
Laser current driver noise	1.2×10^{-14}
Total $\sigma_y(1s) = \sqrt{\sum \sigma_y^2}$	2×10^{-13}

For further investigation, we measured main clock frequency shifts to explain mid-term frequency stability limitations of the CPT-PPOP clock. These studies are detailed in [15]. The latter is presently strongly limited by the laser intensity fluctuations through the light shift effect. Other relevant mechanisms could be the laser frequency variations, the Zeeman shift and length fluctuations of the Michelson delay-line system.

4. Prospects for future improvements

The intermodulation effect is found to be an important contribution to the clock short-term noise budget. A low phase noise microwave synthesizer based on a high-performance 100 MHz oven-controlled quartz oscillator (OCXO) will be implemented nextly on the experiment [16, 17]. This source should allow to reduce the intermodulation effect [18] contribution at the level of about 3×10^{-14} at $\tau = 1$ s, a value closer to the clock shot noise limit.
Laser power fluctuations are a strong limitation to the clock mid-term frequency stability. A proposal to reduce laser intensity effects is to use a Ramsey-type temporal pulsed interrogation [12]. It has been demonstrated that pulsed interaction reduces strongly the intensity-light shift sensitivity [19, 4], prevents the CPT line broadening and allows the detection of narrow and high-contrast Ramsey fringes if combined with optimized CPT pumping schemes [20, 12, 21]. Figure 3 shows an example of a CPT-Ramsey fringe detected with the present setup by making the atoms interact with a light pulsed sequence [20]. The central Ramsey fringe linewidth is here 166 Hz. In pulsed configuration, the clock frequency sensitivity to laser power fluctuations was found to be reduced by a factor of about 10 compared to the CW regime. Further studies are in progress to evaluate the full potential of this technique.
Another way to improve the mid and long term frequency stability of the PPOP Cs CPT clock would be the use of a vapor cell with optimized N_2 - Ar buffer gas mixture for reduced temperature sensitivity of the clock frequency. From [22, 23], a pressure ratio $r = P_{Ar}/P_{N_2} = 0.56$ should allow to shift the inversion temperature close to 35°C.

5. Conclusions

We reported a CPT-based Cs vapor cell atomic clock, using the push-pull optical pumping technique, operating in the continuous regime, with a short-term fractional frequency stability at the level of $3 \times 10^{-13}\ \tau^{-1/2}$ up to $\tau = 100$ s. The short-term and mid-term performances of the clock are presently mainly limited by laser power effects. Further studies and techniques, including Ramsey-type pulsed interrogation or the use of an optimized buffer-gas cell, are under investigation to improve further the clock performances.

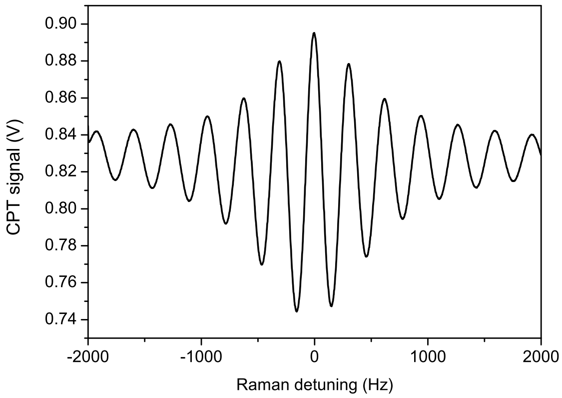

Figure 3. Example of a CPT-Ramsey fringe. The free evolution time is 3 ms. The pumping time is 2 ms. The total laser power incident on the cell is 1.5 mW.

Acknowledgments
This work has been funded by the EMRP program (IND55 Mclocks). The EMRP is jointly funded by the EMRP participating countries within EURAMET and the European Union. This work was partly supported by LNE, LabeX FIRST-TF and ANR-DGA ISIMAC project (ANR-11-ASTR-0004).

References
[1] Vanier J and Mandache C 2007 *Appl. Phys. B* Lasers Opt. **85** DOI: 10.1007/s00340-007-2643-5
[2] Camparo J 2007 *Phys. Today* **60** 11 33
[3] Vanier J 2005 *Appl. Phys. B Lasers Opt.* **81** DOI: 10.1007/s00340-005-1905-3
[4] Micalizio S, Calosso C E, Godone A and Levi F 2012 *Metrologia* **49** 425
[5] Stefanucci C, Bandi T, Merli F, Pellaton M, Affolderbach C, Mileti G and Skrivervik A K 2012 *Rev. Sci. Instrum.* **83** 104706
[6] Kang S, Gharavipour M, Affolderbach C, Gruet F and Mileti G 2012 *Journ. Appl. Phys.* **117** 104510
[7] Boudot R, Guérandel S, De Clercq E, Dimarcq N and Clairon A 2009 *IEEE Trans. Instrum. Meas.* **58** 4 1217
[8] Danet J M, Lours M, Guérandel S and De Clercq E 2014 *IEEE Trans. Ultrason. Ferroelec. Freq. Contr.* **61** 4 567
[9] http://www.inrim.it/Mclocks
[10] Jau Y Y, Miron E, Post A B, Kuzma N N and Happer W 2004 *Phys. Rev. Lett.* **93** 160802
[11] Liu X, Mérolla J M, Guérandel S, Gorecki C, De Clercq E and Boudot R 2013 *Phys. Rev. A* **87** 013416
[12] Liu X, Guérandel S, Mérolla J M, De Clercq E and Boudot R 2013 *Opt. Express* **21** 10 12451
[13] Liu X and Boudot R 2012 *IEEE Trans. Instr. Meas.* **61** 10 2852
[14] http://www.t4science.com/documents/iMaser-Clock-Spec.pdf (iMaser-ST 3000 specifications)
[15] Abdel Hafiz M and Boudot R 2015 *Journ. Appl. Phys.* **118** 124903.
[16] François B, Calosso C E, Danet J M and Boudot R 2014 *Rev. Sci. Instr.* **85** 094709
[17] François B, Calosso C E, Abdel Hafiz M, Micalizio S and Boudot R 2015 *Rev. Sci. Instr.* **86** 094707
[18] Audoin C, Candelier V and Dimarcq N 1991 *IEEE Trans. Instrum. Meas.* **40** 2 121
[19] Castagna N, Boudot R, Guérandel S, De Clercq E, Dimarcq N and Clairon A 2009 *IEEE Trans. Ultrason. Ferroelec. Freq. Contr.* **56** 2 246
[20] Zanon T, Guérandel S, De Clercq E, Holleville D, Dimarcq N and Clairon A 2005 *Phys. Rev. Lett.* **94** 193002
[21] Yun P, Danet J M, Holleville D, De Clercq E and Guérandel S 2014 *Appl. Phys. Lett.* **105** 231106
[22] Kozlova O, Guérandel S and De Clercq E 2011 *Phys. Rev. A* **83** 062714
[23] Kozlova O, Danet J M, Guérandel S and De Clercq 2014 *IEEE Trans. Instr. Meas.* **63**7 1863